Korean J Physiol Pharmacol
Vol 14: 317−324, October, 2010
DOI: 10.4196/kjpp.2010.14.5.317

Regional Distribution of Interstitial Cells of Cajal (ICC) in Human Stomach

Hyo-Yung Yun[1,†,#], Rohyun Sung[2,#], Young Chul Kim[3,*,#], Woong Choi[4,8], Hun Sik Kim[4], Heon Kim[5], Gwang Ju Lee[2], Ra Young You[3], Seon-Mee Park[6], Sei Jin Yun[6], Mi-Jung Kim[7], Won Seop Kim[7], Young-Jin Song[1], Wen-Xie Xu[9], and Sang Jin Lee[3]

Departments of [1]Surgery, [2]Pathology, [3]Physiology, [4]Pharmacology, [5]Preventive Medicine, [6]Internal Medicine, and [7]Pediatrics, College of Medicine, [8]BK21 Chungbuk Biomedical Science Center, School of Medicine, Chungbuk National University, Cheongju 361-763, Korea, [9]Department of Physiology, School of Medicine, Shanghai Jiaotong University, Shanghai 200240, China

We elucidated the distribution of interstitial cells of Cajal (ICC) in human stomach, using cryosection and c-*Kit* immunohistochemistry to identify c-*Kit* positive ICC. Before c-*Kit* staining, we routinely used hematoxylin and eosin (HE) staining to identify every structure of human stomach, from mucosa to longitudinal muscle. HE staining revealed that the fundus greater curvature (GC) had prominent oblique muscle layer, and c-*Kit* immunostaining c-*Kit* positive ICC cells were found to have typical morphology of dense fusiform cell body with multiple processes protruding from the central cell body. In particular, we could observe dense processes and ramifications of ICC in myenteric area and longitudinal muscle layer of corpus GC. Interestingly, c-*Kit* positive ICC-like cells which had morphology very similar to ICC were found in gastric mucosa. We could not find any significant difference in the distribution of ICC between fundus and corpus, except for submucosa where the density of ICC was much higher in gastric fundus than corpus. Furthermore, there was no significant difference in the density of ICC between each area of fundus and corpus, except for muscularis mucosa. Finally, we also found similar distribution of ICC in normal and cancerous tissue obtained from a patient who underwent pancreotomy and gastrectomy. In conclusion, ICC was found ubiquitously in human stomach and the density of ICC was significantly lower in the muscularis mucosa of both fundus/corpus and higher in the submucosa of gastric fundus than corpus.

Key Words: Human stomach, Interstitial cells of Cajal (ICC), c-*Kit*, Fundus, Corpus, Greater and Lesser curvature

INTRODUCTION

Interstitial cell of Cajal (ICC) has long been found in gastrointestinal (GI) tract of animal [1]. It is the end of the last century where researchers began to assume ICC as a regulator of GI motility in animal, including humans, throughout from esophagus to anus [2-6]. Many studies indicated that ICC is the genuine pacemaker cells which generate spontaneous electrical activities, known as slow waves in GI tract [7,8]. Slow waves from ICC spread passively via gap junctions to neighboring GI smooth muscle cells and then produce spontaneous contractions like peristalsis [7-9].

ICC is a myoid cell of mesenchymal origin with pacemaking ability [10]. ICC normally expresses the proto-oncogene c-*Kit*, therefore, antibodies raised against the gene product (c-*Kit*) are useful for the identification of ICC [7,8]. c-*Kit* is a receptor tyrosine kinase, and its activation by ligand [stem cell factor (SCF) or "*Steel*" factor] is essential for the development of ICC. Therefore, a blockade of c-*Kit* with neutralizing antibodies [11] and/or mutations of c-*Kit* or *Steel* [7] impair normal development of ICC in the myenteric plexus region (ICC-MY) of small intestine. It was reported that all subtypes of ICC in human stomach are been developed as early as 4th month developmental stage with their specific functions [4]. To date, at least two types of major ICC have been identified in the GI tract: One is ICC-MY of myenteric region, and the other is a second population of ICC which are distributed outside the myenteric region and is abundant in deep muscular plexus through the muscle layers (intramuscular ICC, ICC-IM). In general, ICC-MY is believed to form two dimensional networks in

Received September 9, 2010, Revised September 24, 2010, Accepted September 28, 2010

*Corresponding to: Young Chul Kim, Department of Physiology, College of Medicine, Chungbuk National University, 12, Gaeshin-dong, Heungduk-gu, Cheongju 361-763, Korea. (Tel) 82-43-261-2859, (Fax) 82-43-261-2859, (E-mail) physiokyc@chungbuk.ac.kr
†Co-corresponding author: Hyo-Yung Yun, Department of Surgery, College of Medicine, Chungbuk National University, 12, Gaeshin-dong, Heungduk-gu, Cheongju 361-763, Korea. (Tel) 82-43-269-6032, (Fax) 82-43-266-6037, (E-mail) yunhyo@chungbuk.ac.kr
#These authors equally contributed to this work.

ABBREVIATIONS: ICC, interstitial cells of Cajal; HE, hematoxylin and eosin; c-*Kit* (+) ICC-like cells, c-*Kit* positive ICC-like cells; GI, gastrointestinal; SCF, stem cell factor; ICC-MY, ICC in the myenteric plexus region; ICC-IM, intramuscular ICC; GIST, gastrointestinal stromal tumor; ICC-SEP, ICC in septa; NANC, non adrenergic and non cholinergic; NO, Nitric oxide.

the neural plexuses and play a role as a pacemaker [7], whereas ICC-IM which is known to occupy only 5% of the tunica muscularis [12] is known to form synaptic connection with nerve terminals of enteric motor neurons of the stomach and play a central role, receptor inputs from motor neurons, although there are still controversies [13-15]. In accordance with this notion, significant reduction of density and constructional destruction of ICC with abnormal functions have been suggested to be responsible for many GI motility disorders and diseases such as constipation, infantile hypertrophic pyloric stenosis and acquired megacolon [16,17]. Indeed, ICC is widely accepted today as an essential target to be considered seriously in many of abnormal GI motility diseases.

In addition to the above mentioned aspect on the motility, ICC has also been shown to be related to inflammatory diseases such as inflammation-induced dysmotility, which is ascribed to damage of ICC [18,19]. In fact, pathophysiological changes of ICC have been reported in GI mucosa and submucosa of diverse gastric diseases such as gastritis and adenocarcinoma [20]. To date, however, only a few studies have attempted to identify and elucidate the role of ICC outside the musculature of the GI tract such as mucosa, microvilli, submucosal plexus and muscularis mucosa [1,21,22]. Furthermore, a mutation of proto-oncogene c-*Kit* has been also reported in a sub-group of GI cancer such as colorectal carcinomas and gastrointestinal stromal tumors (GIST) [23]. c-*Kit* is essential for the maintenance of normal hematopoiesis, melanogenesis and differentiation of mast cell and ICC [24]. Since c-*Kit* is known to maintain their proliferation, migration, and survival [4], the malfunction of c-*Kit* is thought to be associated also with a certain neoplastic disorders and gastric dysmotility in mucosa, microvilli, submucosal plexus and muscularis mucosa [1,21,22]. There is one more type of muscle in muscular layer of human gastric wall, also called oblique muscle, which is more prominent in fundus than corpus. However, physiological role of this muscle and the presence of ICC within the muscle are not yet well understood. Therefore, we first attempted to clarify the distribution of ICC in whole gastric wall, spanning from mucosa through muscularis mucosa, submucosa, oblique muscle, circular muscle, and myenteric plexus to longitudinal muscle. In fact, pathologic changes such as inflammation and carcinogenesis of superficial mucosa and muscularis mucosa might well impair harmonious movement of mucosa and villi in GI tract. Second, we attempted to identify gastric regional differences by classifying stomach to fundus greater curvature, corpus greater curvature and corpus lesser curvature. Since distribution, density and role of ICC in human stomach are not well understood at present, we designed this study to elucidate the distribution of c-*Kit* positive ICC with its density in human stomach.

METHODS

Tissue preparation

Human gastric fundus and corpus from both greater and lesser curvature were obtained from 14 gastric cancer patients who underwent subtotal gastrectomy. Whole thickness samples were taken from the gastric wall of each patient, in particular from the fundus (n=4) and corpus (n=9) of the greater curvature, and the corpus of the lesser curvature (n=1). Specimens were removed from macroscopically normal tissue far from the neoplastic area immediately after surgical operation. All patients gave written informed consent and this experimental protocol using human stomach was also approved by the Institutional Review Board for Clinical Research of Chungbuk National University, School of Medicine, Korea. Specimens in Krebs-Ringer bicarbonate (KRB) solution were pinned on sylgard plate in order to maintain original shape and length. Then, connective tissues were removed, cut and pinned to rectangular shape (2×3 cm, width and length). Finally, these gastric tissues were fixed in 4% paraformaldehyde in 0.1 M sodium phosphate buffer for 24 hours at room temperature (RT). Two longitudinal sections, 3 cm in length and 3 mm in thickness, were taken from each fixed tissue. The sections were processed on a computerized tissue processor (Tissue-Tek VIP; Sakura Finetek, Torrance, CA, USA) and embedded in paraffin (Paraplast Medium; Leica Biosystems, Maarn, The Netherlands) on a tissue embedding console system (Tissue-Tek TEC; Sakura Finetek, Torrance, CA, USA). Five formalin-fixed paraffin tissue blocks were also retrieved from the archive of the Pathology Department at Chungbuk National University Hospital. They consisted of one tissue block from normal corpus of the stomach, resected at Whipple operation for pancreas adenocarcnoma, and four tissue blocks from gastric adenocarcinoma resected at subtotal or total gastrectomy.

All paraffin embedded tissue blocks were sectioned at 4 μm thickness with a microtome, and slides were then prepared. Paraffin was removed from the slides with xylene treatment. The sections were rehydrated with an ethanol series and stained with hematoxylin and eosin. Final stages of processing were performed with an automated slide stainer (Tissue-Tek Prisma; Sakura Finetek, Torrance, CA, USA) and automated coverslipper (Tissue-Tek Glas; Sakura Finetek, Torrance, CA, USA).

Immunohistochemical labeling of interstitial cells of Cajal (ICC) by c-Kit

Sections from paraffin embedded gastric tissues were cut at 4 μm thickness and mounted on positively charged slides (Superfrost Plus; VWR Internatinal, West Chester, PA, USA). Deparaffinization and antigen retrieval prior to immunostaining were simultaneously accomplished on an automated PT module (Lab Vision, Fremont, CA, USA). Immunohistochemistry was done on an automated immunostainer (Autostainer 360; Lab Vision, Fremont, CA, USA) according to the manufacturer's protocol. Peroxidase staining was done using UltraVision LP Detection System HRP Polymer & DAB Plus Chromogen (Thermo Fisher Scientific, Fremont, CA, USA). Briefly the sections were incubated in hydrogen peroxide block for 10 minutes to reduce nonspecific background staining due to endogenous peroxidase. After washing in phosphate buffered saline plus Tween 20 (20×) (PBS; ScyTek laboratories, Logan, Utah, USA), they were incubated with ultra V block for 5 minutes at RT to block nonspecific binding. The sections were then incubated with polyclonal rabbit anti-human CD117 (Dako, Carpinteria, CA, USA) at a dilution of 1 : 400 and monoclonal mouse anti-human mast cell tryptase (clone AA1; Dako, Glostrup, Denmark) at a dilution of 1 : 200 for 40 minutes at RT. After washing in PBS, they were incubated at RT with primary antibody enhancer, followed by washes in PBS and incubation with the HRP polymer for 15 minutes at RT. Sections were then washed in PBS, followed

by staining with DAB Plus Chromogen and Substrate. Counterstaining was performed with hematoxylin. Negative controls were prepared by omitting primary antibodies or by substituting them with a nonimmune serum in order to check the specificity of the immunostaining. All sections for histologic and immunohsitochemical analysis were examined using a microscope (BX50; Olympus Corporation), and photographs were taken with attached camera (ProgRes C14; JENOPTIK, Jena, Germany) operated with CapturePro software (JENOPTIK, Jena, Germany).

Solution and drugs

KRB solution (CO_2/bicarbonate-buffered Tyrode) contained (in mM): NaCl 122, KCl 4.7, $MgCl_2$ 1, $CaCl_2$ 2, $NaHCO_3$ 15, KH_2PO_4 0.93, and glucose 11 (pH 7.3~7.4, bubbled with 5% CO_2/95% O_2). PBS was purchased from ScyTek laboratories (USA). All drugs used in this study were purchased from Dako (anti-human c-*Kit*, anti-human mast cell tryptase) and Sigma.

Statistics

The data are expressed as means±SEM. Statistical significance was estimated by Student's *t*-test. $p<0.05$ was considered to be statistically significant.

RESULTS

The histology of human stomach in hematoxylin and eosin (HE) staining

Fig. 1A shows histology of three regions (fundus greater curvature, corpus greater curvature and corpus lesser curvature) of human stomach. In Fig. 1Ba, we could identify muscle layers of oblique, circular and longitudinal muscle in greater curvature of fundus. As shown in Fig. 1Ba and 1Bb, we routinely identified whole structure of stomach first by HE staining before immunohistochemical analysis and then compared it to the structure revealed by c-*Kit* immunoreactivity. From these stainings, we verified that oblique muscle layer was more prominent in gastric fundus than gastric corpus in human stomach (Fig. 1B, 2, 3, 4, 5B and 5C). c-*Kit* positive immunoreactivity was observed in every layer of all three regions in human stomach.

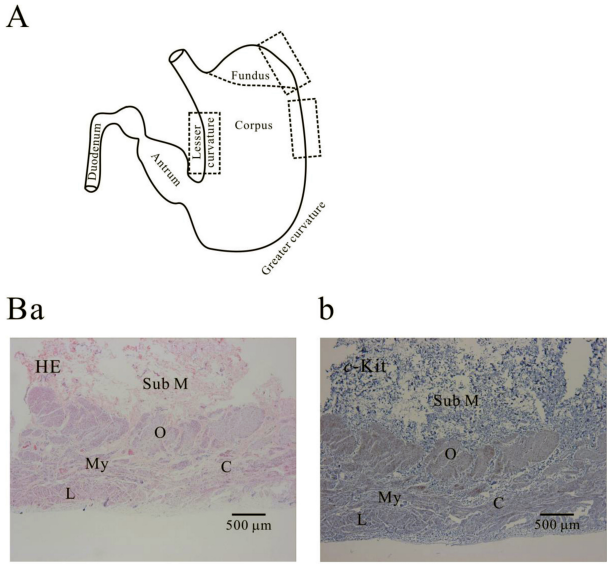

Fig. 1. Histology of human gastric wall. As shown in panel A, we used fundus greater curvature, corpus greater curvature and corpus lesser curvature of human stomach. In HE staining of fundus greater curvature (Ba), we identified oblique, circular and longitudinal muscles. And then in c-*Kit* immunostaining (Bb), we observed c-*Kit* positive immnuhistochemical reactivity of ICC, which appeared as dark brown spots. Sub M, submucosa; O, oblique muscle; C, circular muscle; My, myenteric region; L, longitudinal muscle.

Distribution of ICC in human gastric fundus

HE-stained structure of human gastric fundus was compared with that of c-*Kit* immunoreactivity. As shown in Fig. 2 and 4A, c-*Kit* positive ICC was observed, ranging from muscularis mucosa all the way to longitudinal muscle layer

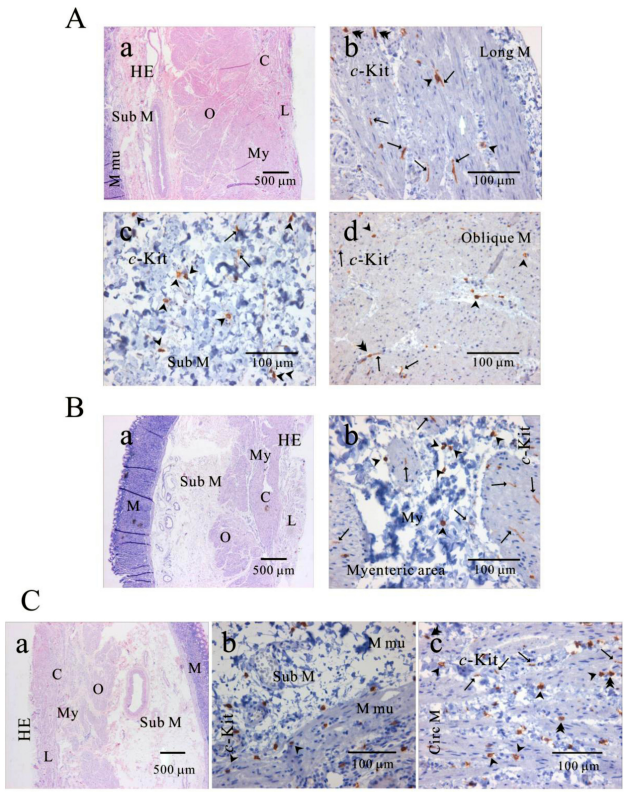

Fig. 2. Distribution of ICC in human gastric fundus of greater curvature. In HE staining (Aa, Ba, Ca), the whole layers of human gastric fundus from greater curvature can be seen. Oblique muscle layer is prominent in human gastric fundus. In c-*Kit* immunostaining, we identified c-*Kit* positive ICC in every muscle layers: longitudinal muscle (Ab), submucosa (Ac), oblique muscle (Ad), myenteric area (Bb), muscularis mucosa (Cb) and circular muscle (Cc). Since we used cryosection for immunohistochemical study, ICC could not be seen as a whole structure. Instead, ICC is seen in long spindle-like (fusiform) shaped cell body and multiple processes from the central cell body, which is especially prominent in (Ab, Ad, Bb). ICC is identified in submucosa, muscularis mucosa and mucosa, too (Ac) and (Cb). Arrow: processes or ramification, arrow head: central cell body, double arrow head: ICC in septa (ICC-SEP).

in fundus of greater curvature. In each layer, long spindle-like (fusiform) cell body (arrow head) with multiple processes (arrow) protruded from the central cell body was observed (Fig. 2, 4A and 5A). ICC in septa (ICC-SEP) is indicated by double arrow head. In oblique muscle (Fig. 4Ad) and myenteric border (Fig. 4Af) of human gastric fundus, we could observe typical ICC maintaining fusiform cell body and attached processes together. However, we could not generally identify whole ICC morphology, because we sliced the tissue using cryosection for c-*Kit* immunostaining. Therefore, dotted dark brown cells with nucleus or individual processes such as dark brown rod are c-*Kit* positive immunoreactivity usually found, although ICC forms network in fact. In this study, nevertheless, we clearly demonstrated c-*Kit* positive ICC of muscularis mucosa (Fig. 2Cb, 3Ab, 4Ab, 4Bb and 5Ab). Since ICC in the muscularis mucosa has been reported only in one or two animal studies, the present finding is valuable, showing the possibility that ICC might play a role for harmonious movement of mucosa and microvilli.

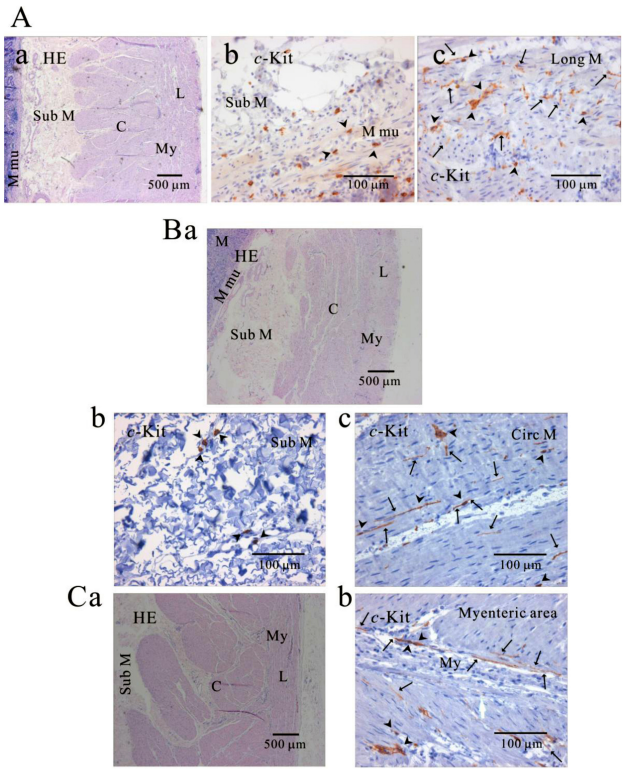

Fig. 3. Distribution of ICC in human gastric corpus of greater curvature. In HE staining (Aa, Ba, Ca), the whole layers of human gastric corpus from greater curvature can be seen. In c-*Kit* immunostaining, c-*Kit* positive ICC is also observed in every layer; muscularis mucosa (Ab), longitudinal muscle (Ac), submucosa (Bb), circular muscle (Bc), and myenteric area (Cb). In human gastric corpus, oblique muscle is not as prominent as in fundus. ICC is seen in long spindle-like (fusiform) shaped cell body and multiple processes from the central cell body, and is also identified in mucosa (Ab). Arrow: processes or ramification, arrow head: central cell body.

Distribution of ICC in human gastric corpus

As shown in Fig. 3, 4B, 5A and 5C, c-*Kit* positive ICC was observed also in every layer of muscularis mucosa, all the way to longitudinal muscle layer in gastric corpus of both greater and lesser curvature. Fusiform cell bodies and multiple processes from them were observed, as shown in Fig. 3Ac, 3Bc, 3Cb, 4Bd, 4Be and 4Bf. In circular muscle, myenteric border and longitudinal muscle (*Bf inset*) of gastric corpus, long spindle-like cell bodies, processes and even numerous ramifications arising from cell processes were observed, as shown in Fig. 4Bb, 4Bd, 4Be, 3Cb, and 3Ac. Fig. 5A shows ICC of gastric corpus from lesser curvature. In corpus lesser curvature, c-*Kit* positive ICC was found also in all the layers examined.

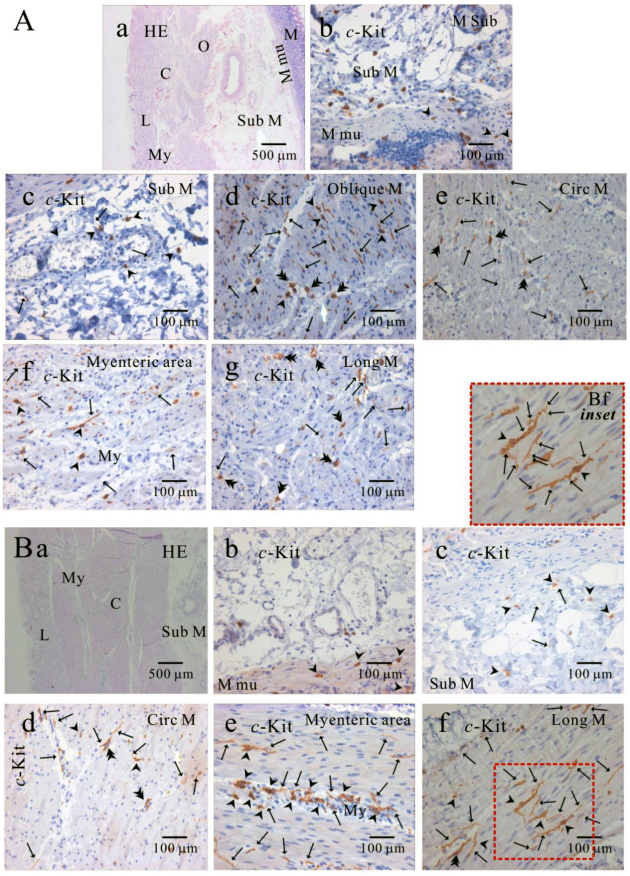

Fig. 4. Comparison of histology between fundus and corpus in greater curvature of human stomach. In HE staining, the whole layer of fundus (Aa) and corpus (Ba) are shown. It is striking to find that fundus has prominent structure of oblique muscle, unlike corpus. c-*Kit* positive ICC is observed in every layer of human gastric fundus (Ab～Ag) and corpus (Bb～Bf) of greater curvature. Interestingly, almost all kinds of ICC are found in oblique muscle layer, however, ICCs of circular and longitudinal muscle are ICC-SEP. In *panel* (Bf and Bf *inset*), it is evident that ICC of longitudinal muscle has lots of processes and ramifications. Arrow: processes or ramification, arrow head: central cell body, double arrow head: ICC in septa (ICC-SEP).

Comparison of ICC distribution between fundus and corpus

Since we could not get enough number of gastric tissues from lesser curvature, the distribution of ICC was compared between fundus (Fig. 5B) and corpus (Fig. 5C) from greater curvature of human stomach. We counted dense cell body with nucleus as one individual ICC under 400× magnification field of microscopy, and the number of ICC twice under double or three side-viewed microscopy together and then averaged it for quantitative analysis. In fundus greater curvature, the averaged number of ICC of muscularis mucosa, submucosa, oblique muscle, circular muscle, myenteric border and longitudinal muscle were 1.7±0.9, 8±0.7, 6±3, 4.8±1.9, 6.3±0.5, 4.9±1.2, rescpectively (n=3, 4, 2, 4, 4 and 4, respectively; Fig. 5A). In corpus greater curvature, the averaged number of ICC of muscularis mucosa, submucosa, circular muscle, myenteric border and longitudinal muscle were 2.3±0.5, 4.1±0.7, 5.1±1.0, 4.3±0.6, 3.8±0.4, respectively (n=8, 10, 10, 10 and 10, respectively; Fig. 5B). In fundus and corpus of stomach, the density of ICC in muscularis mucosa was significantly less than that of other layers of fundus (submucosa and myenteric area) and corpus (circular muscle, myenteric area and longitudinal muscle) ($p < 0.05$; Fig. 5B and 5C). Meanwhile, the density of ICC in muscularis mucosa was less than other layers (fundus oblique, circular and longitudinal muscle, and corporal sub mucosa), but with no significant difference ($p > 0.05$; Fig. 5B and 5C).

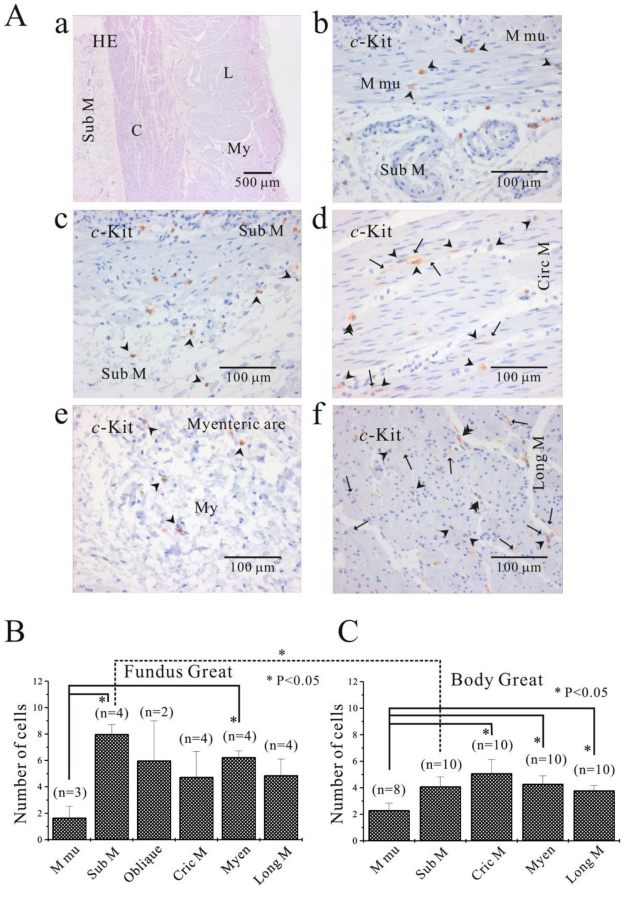

Fig. 5. Comparison of ICC distribution between corpus and fundus and regional distribution of ICC in part of human stomach. In HE staining (Aa), the whole layers of human gastric corpus from lesser curvature are demonstrated. In corpus lesser curvature, c-*Kit* positive ICC is also found in all the layers (A). ICC numbers are compared between fundus greater curvature (B) and corpus greater curvature (C). There is no significant difference between two regions except for ICC from submucosa. The average number of ICC is 8±0.7 count/unit area in submucosa of fundus greater curvature, which is significantly higher than 4.1±0.7 count/unit area of body greater curvature ($p < 0.05$). Meanwhile, the density of ICC in muscularis mucosa is significantly less than that of other layers of fundus (submucosa and myenteric area) and corpus (circular muscle, myenteric area and longitudinal muscle) ($p < 0.05$; (5B) and (5C)). However, the density of ICC in muscularis mucosa is less than that of other layer with no significant difference ($p > 0.05$; (5B) and (5C)). Arrow: processes or ramification, arrow head: central cell body, double arrow head: ICC in septa (ICC-SEP).

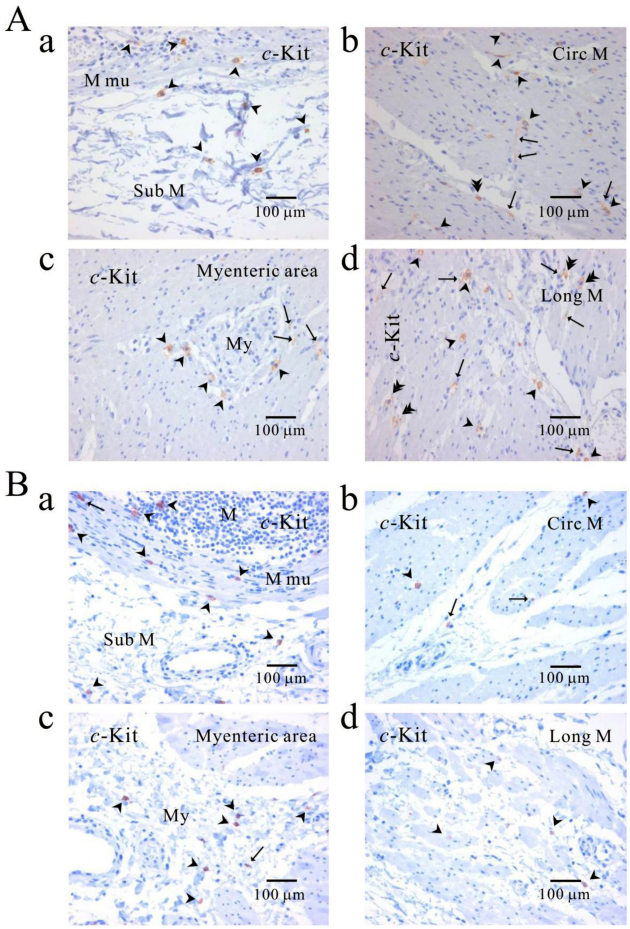

Fig. 6. Comparison of ICC distribution between normal and cancerous tissue of human stomach. Distribution of ICC is compared between normal (A) and cancerous tissue (B) obtained from a patient who underwent pancreotomy and gastrectomy. c-*Kit* positive ICC is observed in every layer; submucosa (Aa, Ba), circular muscle (Ab, Bb), myenteric area (Ac, Bc), and longitudinal muscle (Ad, Bd). Note that c-*Kit* positive immunoreactivity is found also in gastric mucosa of cancer area (Ba) as well as normal area (Aa). Arrow: processes or ramification, arrow head: central cell body, double arrow head: ICC in septa (ICC-SEP).

Furthermore, no significant difference was observed between two regions except for ICC from submucosa. The averaged number of ICC in submucosa from fundus greater curvature was significantly higher than that from corpus greater curvature ($p < 0.05$; Fig. 5B and 5C).

Comparison of ICC distribution between normal and cancerous tissue

Distribution of ICC was compared between the corpus (Fig. 6A) of normal person and cancerous tissue (Fig. 6B) obtained from a patient who underwent pancreotomy and gastrectomy. c-*Kit* positive ICC was observed in every layer. c-*Kit* positive immunoreactive ICC was found also in gastric mucosa of cancer area as well as normal area.

The c-Kit positive cells in human gastric mucosa

As shown in Fig. 2Cb, 3Ab, 4Ab, 6Aa and 6Ba, c-*Kit* positive immunoreactivity was found in all the mucosae from three regions. In addition, ICC was found in cancer area. It was of an interest to find c-*Kit* positive ICC-like cells [c-*Kit* (+) ICC-like cells] and they have been suggested to be involved in inflammation, dysplasia and tumorigenesis in human stomach (*see discussion*).

DISCUSSION

In the present study, we investigated the distribution of c-*Kit* positive ICC in fundus greater curvature, corpus greater curvature and corpus lesser curvature of human stomach to determine whether they show regional variations of ICC density along the circumference and along the length in the organ. The results showed that ICC was distributed in every layer of gastric wall in decreasing order of mucosa, muscularis mucosa, submucosa, oblique muscle, circular muscle, myenteric region, longitudinal muscle. There was no significant difference in the density of ICC between fundus and corpus except for ICC in submucosa. The density of ICC in submucosa of fundus was higher than that of corpus, and the density of ICC in muscularis mucosa of each fundus and corpus was significantly lower than other layers.

As well known, ICC expresses a proto-oncogene c-*Kit* [4]. However, except for marker for ICC, c-*Kit* and/or SCF have been shown to be expressed also in variety of normal tissues such as brain, placenta and lung [25] as well as malignant tumors and gastric carcinoma cell line [20,26]. In addition, activation of c-*Kit* by mutations has been shown also in a number of human malignancies such as human gastric carcinomas [20,27], gastrointestinal GIST [23], small cell lung cancer [26], and colorectal cancer [23]. Therefore, ICC seems to have many abilities, and it might be associated also with tumor growth and/or the process of carcinogenesis in gastric mucosa. Although data are not shown here, we also found c-*Kit* positive ICC-like cells [c-*Kit* (+) ICC-like cells] which are associated with inflammation and/or regeneration of epithelium in human stomach (manuscript *in submission*). We confirmed the existence of c-*Kit* (+) ICC-like cells in human gastric mucosa: They are present mainly in the stroma around repair zone of the glands in chronic gastritis as well as in normal mucosa, whereas they seem to redistribute over the entire mucosa in gastritis with intestinal metaplasia. c-*Kit* (+) ICC-like cells around repair zone are found tightly attached to epithelial cells, but not to metaplastic epithelial cells. Thus, c-*Kit* (+) ICC-like cells seem to have a role in epithelial recovery process, and may even be associated with carcinogenesis of human gastric mucosa (manuscript *in submission*). Further study is in progress to get more evidences.

Near the end of the last century, ICC was suggested to be a regulator of GI motility in animals, including humans, throughout from esophagus to anus [2,3,6], and the distribution was found not even in stomach, small intestine and colon, showing regional differences. For example, the density of ICC-MY was higher at antrum and corpus than at fundus in murine stomach, whereas ICC-IM was denser at fundus and corpus than at antrum [28]. Furthermore, the density of ICC-IM was lower at lesser curvature than greater curvature within the same corpus region [28,29], and the density of ICC-IM was much higher at circular muscle layer than at longitudinal muscle layer within muscle coat. Therefore, the regional unique distribution of ICC seemed to be related to unique physiological function of each GI tract. In fact, the density of ICC in colon was much higher at proximal colon, where strong haustral contractions toward anus begin [30]. Recently, ICC was reported also in human stomach, small intestine and colon [15,31,32], and all subtypes of ICC were shown to develope as early as 4^{th} month development stage [4]. However, still little is known on the regional variation of ICC in human stomach. In the present study, therefore, we attempted to elucidate the distribution of ICC in fundus greater curvature, corpus great curvature and corpus lesser curvature. In fundus and corpus of great curvature, ICC was observed in every layers in decreasing order of mucosa, muscularis mucosa, submucosa, circular muscle, myenteric area, and longitudinal muscle. Only in submucosa layer, ICC density of fundus greater curvature was higher than that of corpus greater curvature (Fig. 5B and 5C), and the density of ICC in muscularis mucosa of each fundus (compared to that of submucosa and myenteric region) and corpus (compared to circular muscle, myenteric region and longitudinal muscle) was also significantly lower than other layers (Fig. 5B and 5C). In the case of oblique muscle, as already known, fundus showed prominently thick oblique muscle layer (Fig. 1A, 2, 3A and 5B), where ICC was overexpressed (Fig. 4Ad). This finding seems to coincide with the report that ICC is overexpressed in muscular hypertrophy. We plan to address on this finding in the future.

There are species differences and regional variations in the morphology and distribution of ICC of GI tract. ICC of bipolar type has been identified in muscle coat of mouse and guinea-pig [13,33] and in fundus of human fetus [6], whereas multipolar type has been reported in myenteric border of corpus and antrum of mouse and guinea-pig [13, 33]. ICC in rat and dog antrum is all bipolar type [34]. In the present study, we failed to find out exactly how many types of ICC were present in human stomach. Nonetheless, we found some regional differences in density of processes and ramifications of ICC. The processes and ramifications of ICC of corpus greater curvature were more prominent in myenteric area (Fig. 3Cb vs Fig. 2Bb, Fig. 4Be vs Fig. 4Af) and longitudinal muscle layer (Fig. 3Ac vs Fig. 2Ab, Fig. 4Bf vs Fig. 4Ag; see inset of Fig. 4Bf) compared with those of fundus greater curvature. The oblique muscle layer was significantly prominent only in fundus, however, did not show consistent result (Fig. 2Ad vs Fig. 4Ad). The corpus lesser curvature did not show much process and ram-

ifications (Fig. 5). The study using cryosection seems to have a limitation in elucidating whole morphology of ICC cells.

In addition to the morphology of ICC, the distribution of ICC has been known to show regional and species differences in animals such as human [31] and dog [34]. In human stomach, ICC was reported to be present at the border of submucosa in antrum [35], but absent in the inner part of the corporal circular muscle layer [31]. In the present study, however, we observed ICC practically everywhere, particularly dense in submucosa (Fig. 2Ac, Fig. 3Ab, Fig. 4Ab, Fig. 4Ac, Fig. 4Bc and Fig. 5Ac). We showed the existence of intramuscular ICC in muscle layers of oblique (Fig. 4d, corpus), circular (Fig. 3Bc, corpus) and longitudinal muscles without significant difference in their distribution (Fig. 2Ab, fundus; Fig. 3Ac and Fig. 4Bf, corpus). ICC in septa (ICC-SEP) was reported only in corpus and antrum in human and animal stomach [34,35], however, we found ICC-SEP in fundus (Fig. 4Ae, circular muscle; Fig. 4Ag, longitudinal muscle), corpus (Fig. 4Bd, circular muscle), and corpus lesser curvature (Fig. 5A).

In the present study, we found ICC in every layer of fundus including myenteric region (Fig. 2, 4A, 5B). In GI tract, spontaneous contraction is ascribed to pacemaking potential generated by ICC-MY. However, fundus does not show spontaneous motility and has ICC-MY in myenteric border of mouse and guinea-pig [13,33]. Recently, Kim et al. found spontaneous contraction in fundus smooth muscle of human stomach, and circular and longitudinal muscles showed rhythmical spontaneous contraction, respectively (manuscript *in submission*). However, spontaneous contractility almost disappeared by stepwise increment of isotonic load to 1 g (data not shown). Gastric fundus plays a storage function called gastric receptive relaxation via vagally mediated mechanism [36]. The gastric fundus is innervated by both excitatory cholinergic neurons and NANC (non adrenergic- and non cholinergic) inhibitory neurons, which are associated with gastric receptive relaxation [36]. Nitric oxide (NO) has been recognized as an inhibitory neurotransmitter to mediate smooth muscle relaxation in the mammalian gastrointestinal tract. All these results imply that the basic role of fundus is passive relaxation. Therefore, spontaneous contractility of fundus observed in this study was somewhat unexpected. In fact, ICC has already been shown to exist in human fundus including myenteric area [31,35]: it was pointed out that the difference between human and mouse and guinea-pig was due to the presence of ICC-MY in myenteric border. The above finding is consistent with our present data, since we also found ICC-MY in human gastric fundus (Fig. 2, 4A and 5B). Therefore, the ICC might be responsible for the spontaneous rhythmicity of circular and longitudinal smooth muscle of human gastric fundus. Since it produced spontaneous motility in resting state and disappeared in stretched state, it is highly likely that spontaneous rhythmicity would disappear after food intake to serve as a reservoir, and that spontaneous rhythmicity in time would return to help propel food, taken by receptive relaxation, or remain in fundus to gradually distal stomach.

In this study, we found also c-*Kit* positive cells in submucosa and muscularis mucosa in human gastric fundus and corpus. Recently, ICC associated with submucosal plexus (ICC-SP) was found in guinea-pig stomach, seemingly contributing to the regulation of the mucosal function such as secretion, absorption and transportation of fluid [21]. In accordance with pacemaker activity of muscularis mucosa, the spontaneous pacemaking motility was reported earlier in rabbit stomach (4.55～4.70 cycles/min) [37]. In fact, the spontaneous motility of muscularis mucosa might also be ascribed to glandular pressure and red blood cell velocity, even in humans [38], and it could regulate the amount of blood in gastric mucosal venous system [39]. These reciprocal changes might alter the intramucosal pressure, thus affecting the movement of tissue fluid and the function of the gastric cells indirectly. To date, ICC-like cells in muscularis mucosa was reported also in rat stomach including pacemaking response [19,37]. In addition, ICC-SP has a close structural relationship with the muscle fibers of the muscularis mucosa, therefore, they may also be functionally involved in villous movement. In fact, although the presence of ICC-SP in the small intestine has not yet been demonstrated, muscle bundles within the villi are known to be continuous with those of the muscularis mucosa, and nerve fibers from the submucous plexus innervate the muscularis mucosa and smooth muscle fibers in the cores of the intestinal villi [40]. Since ICC-SP and ICC were found in muscularis mucosa of human stomach in this study, they might possibly be associated with spontaneous villous movement and physiological function of gastric mucosa. In this study, we found that the density of submucosal ICC in fundus greater curvature was significantly higher than that of corpus greater curvature ($p < 0.05$; Fig. 5B and C). Since gastric acid is secreted from fundus gastric glands, the ICC of submucosa and muscularis mucosa of fundus might well be related to increased activity of secretion through coordination of mucosal and/or villous movement.

ACKNOWLEDGEMENT

This work was supported by the research grant of the Chungbuk National University in 2008.

REFERENCES

1. **Cajal SR.** Histologie du système nerveux de l'homme et des vertébrés. 2nd ed. Paris: Maloine; 1911. 891-942 p.
2. **Faussone-Pellegrini MS, Cortesini C.** Ultrastructural features and localization of the interstitial cells of Cajal in the smooth muscle coat of human esophagus. *J Submicrosc Cytol.* 1985;17: 187-197.
3. **Hagger R, Gharaie S, Finlayson C, Kumar D.** Regional and transmural density of interstitial cells of Cajal in human colon and rectum. *Am J Physiol.* 1998;275:G1309-G1316.
4. **Radenkovic G, Savic V, Mitic D, Grahovac S, Bjelakovic M, Krstic M.** Development of c-*Kit* immunopositive interstitial cells of Cajal in the human stomach. *J Cell Mol Med.* 2010;14:1125-1134.
5. **Romert P, Mikkelsen HB.** c-*Kit* immunoreactive cells of Cajal in the human small and large intestine. *Histochem Cell Biol.* 1998;109:195-202.
6. **Torihashi S, Horisawa M, Watanabe Y.** c-*Kit* immunoreactive interstitial cells in the human gastrointestinal tract. *J Auton Nerv Syst.* 1999;75:38-50.
7. **Huizinga JD, Thuneberg L, Kluppel M, Malysz J, Mikkelsen HB, Bernstein A.** W/Kit gene required for interstitial cells of Cajal and for intestinal pacemaker activity. *Nature.* 1995;373: 347-349.
8. **Torihashi S, Ward SM, Sanders KM.** Development of c-*Kit*-positive cells and the onset of electrical rhythmicity in murine small intestine. *Gastroenterology.* 1997;112:144-155.
9. **Nemeth L, Maddeur S, Puri P.** Immunolocalization of the gap

junction protein connexin 43 in the interstitial cells of Cajal in the normal and Hirschsprung's disease bowel. *J Pediatr Surg.* 2000;35:823-828.
10. **Klüppel M, Huizinga JD, Malysz J, Bernstein A.** Developmental origin and Kit- dependent development of the interstitial cells of Cajal in the mammalian small intestine. *Dev Dyn.* 1998;211: 60-71.
11. **Maeda H, Yamagata A, Nishikawa S, Yoshinaga K, Kobayashi S, Nishi K, Nishikawa S.** Requirement of c-*Kit* for development of intestinal pacemaker system. *Development.* 1992;116:369-375.
12. **Ördög T, Redelman D, Horváth VJ, Miller LJ, Horowitz B, Sanders KM.** Qunatitative analysis by flow cytometry of interstitial cells of Cajal, pacemakers, and mediators of neurotransmission in the gastrointestinal tract. *Cytometry A.* 2004; 62:139-149.
13. **Burns AJ, Lomax AE, Torihashi S, Sanders KM, Ward SM.** Interstitial cells of Cajal mediated inhibitory neurotransmission in the stomach. *Proc Natl Acad Sci USA.* 1996;93:12008-12013.
14. **Goyal RK, Chaudhury A.** Mounting evidence against the role of ICC in neurotransmission to smooth muscle in the gut. *Am J Physiol Gastrointest Liver Physiol.* 2010;298:G10-G13.
15. **Wang XY, Paterson C, Huizinga JD.** Cholinergic and nitrergic innervation of ICC-DMP and ICC-IM in the human small intestine. *Neurogastroenterol Motil.* 2003;15:531-543.
16. **Nakahara M, Isozaki K, Hirota S, Vanderwinden JM, Takakura R, Kinoshita K, Miyagawa J, Chen H, Miyazaki Y, Kiyohara T, Shinomura Y, Matsuzawa Y.** Deficiency of Kit-positive cells in the colon of patients with diabetes mellitus. *J Gastroenterol Hepatol.* 2002;17:666-670.
17. **Vanderwinden JM, Rumessen JJ.** Interstitial cells of Cajal in human gut and gastrointestinal disease. *Microsc Res Tech.* 1999;47:344-360.
18. **Der T, Bercik P, Donnelly G, Jackson T, Berezin I, Collins SM, Huizinga JD.** Interstitial cells of Cajal and inflammation-induced motor dysfunction in the mouse small intestine. *Gastroenterology.* 2000;119:1590-1599.
19. **Popescu LM, Gherghiceanu M, Cretoiu D, Radu E.** The connective connection: interstitial cells of Cajal-like cells establish synapses with immunoreactive cells. *J Cell Mol Med.* 2005;9: 714-730.
20. **Hassan S, Kinoshita Y, Kawanami C, Kishi K, Matsushima Y, Ohashi A, Funasaka Y, Maekawa T, He-Yao W, Chuba T.** Expression of protooncogene c-*Kit* and its ligand stem cell factor (SCF) in gastric carcinoma cell lines. *Digestive Diseases and Sciences.* 1998;43:8-14.
21. **Kunisawa Y, Komuro T.** Interstitial cells of Cajal associated with submucosal plexus of the guinea-pig stomach. *Neuroscience Letters.* 2008;434:273-276.
22. **Torihashi S, Yokoi K, Nagaya H, Aoki K, Fujimoto T.** New monoclonal antibody (AIC) identifies interstitial cells of Cajal in the musculature of the mouse gastrointestinal tract. *Auton Neurosci.* 2004;113:16-23.
23. **Reed J, Ouban A, Schickor FK, Muraca P, Yeatman T, Coppola D.** Immunohistochemical staining for c-*Kit* (CD117) is a rare event in human colorectal carcinoma. *Clin Colorectal Cancer.* 2002;2:119-122.
24. **Ashman LK.** The biology of stem cell factor and its receptor C-*kit*. *Int J Biochem Cell Biol.* 1999;31:1037-1051.
25. **Rygaard K, Nakamura T, Spang Thomsen M.** Expression of the proto-oncogene c-met and c-*Kit* and their ligands, hepatocyte growth factor/scatter facter and stem cell factor, in SCLS cell lines and xenografts. *Br J Cancer.* 1993;67:37-46.
26. **Hibi K, Takahashi T, Sekido Y, Ueda R, Hida T, Ariyoshi Y, Takagi H, Takahashi T.** Coexpression of the stem cell factor and the c-*Kit* genes in small-cell lung cancer. *Oncogene.* 1991;6: 2291-2296.
27. **Fujiwara T, Motoyama T, Ishihara N, Watanabe H, Kumanishi T, Kato K, Ichinose H, Nagatsu T.** Characterization of four new cell lines derived from small-cell gastrointestinal carcinoma. *Int J Cancer.* 1993;54:965-971.
28. **Song G, Hirst GDS, Sanders KM, Ward SM.** Regional variation in ICC distribution, pacemaking activity and neural responses in the longitudinal muscle of the murine stomach. *J Physiol.* 2005;564:523-540.
29. **Hirst GDS, Beckett EAH, Sanders KM, Ward SM.** Regional variation in contribution of myenteric and intramuscular interstitial cells of Cajal to generation of slow waves in mouse gastric antrum. *J Physiol.* 2002;540:1003-1012.
30. **Han J, Shen WH, Jiang YZ, Yu B, He YT, Mei F.** Distribution, development and proliferation of interstitial cells of Cajal in murine colon: an immunohistochemical study from neonatal to adult life. *Histochem Cell Biol.* 2010;133:163-175.
31. **Ibba Manneschi L, Pacini S, Corsani L, Cechi P, Faussone-Pellegrini MS.** Interstitial cells of Cajal in the human stomach: distribution and relationship with enteric innervation. *Histol Histopathol.* 2004;19:1153-1164.
32. **Nemeth L, Puri P.** Three-demensional morphology of c-*Kit*-positive cellular network and nitrergic innervation in the human gut. *Arch Pathol Lab Med.* 2001;125:899-904.
33. **Burns AJ, Herbert TM, Ward SM, Sanders KM.** Interstitial cells of Cajal in the guinea-pig gastrointestinal tract as revealed by c-*Kit* immunohistochemistry. *Cell Tissue Res.* 1997;290:11-20.
34. **Horiguchi K, Sanders KM, Ward SM.** Enteric motor neurons from synaptic-like junctions with interstitial cells of Cajal in the canine gastric antrum. *Cell Tissue Res.* 2003;311:299-313.
35. **Faussone-Pellegrini MS, Pantalone D, Cortesini C.** An ultrastructural study of the interstitial cells of Cajal of the human stomach. *J Submicrosc Cytol Pathol.* 1989;21:439-460.
36. **Abrahamsson H.** Studies on the inhibitory nervous control of gastric motility. *Acta Physiol Scand Suppl.* 1973;390:1-38.
37. **Percy WH, Warren JM, Brunz JT.** Characteristics of the muscularis mucosae in the acid-secreting region of the rabbit stomach. *Am J Physiol.* 1999;276:G1213-G1220.
38. **Synnerstad I, Ekblad E, Sundler F, Holm L.** Gastric mucosal smooth muscles may explain oscillations in glandular pressure: role of vasocative intestinal peptide. *Gastroenterology.* 1998; 114:284-294.
39. **Moskalewski S, Biernacka-Wawrzonek D, Klimkiewicz J, Zdun R.** Venous outflow system in rabbit gastric mucosa. *Folia Morphol (Warsz).* 2004;63:151-157.
40. **Fawcett DW.** A Textbook of Histology. 12th ed. New York, London: Chapman & Hall; 1994. 617-651 p.